Paper

Ultra-wideband 3D image processing for improving landmine detection with GPR

Eveline E. Ligthart, Alexander G. Yarovoy, Friedrich Roth, and Leo P. Ligthart

Abstract—This paper describes a new landmine detection algorithm starting from high resolution 3D ground penetrating radar (GPR) images. The algorithm consists of two procedures, object detection and object classification; both strongly depend on the properties of 3D GPR images. The algorithm has been tested on data measured with an ultra-wideband (UWB) video impulse radar (VIR) system developed by the International Research Centre for Telecommunications and Radar (IRCTR). It was found that the algorithm is able to detect all landmines (including difficult to detect M14 mines) and classifies almost all landmines correctly with a large reduction in the number of false alarms caused by clutter. It turns out that for clutter removal it is most effective to eliminate detected objects with a small height.

Keywords— ground penetrating radar, image processing, object detection, classification, clutter removal.

1. Introduction

Improving detectability and decreasing the false alarm rate of a ground penetrating radar (GPR) sensor for landmine detection is the main objective of numerous researches in the past years. Some improvements can be obtained in software processing, particularly for mine detection in GPR images, by optimising image processing techniques. The contribution of this paper lies in reducing the false alarm rate and obtaining a better performance than existing methods in GPR landmine detection.

Earlier research on object detection has been performed. In [1], landmines have been detected using an 2D energy projection of a synthetic aperture radar (SAR) image volume. Also research of object detection and classification of landmines in 2D images has been performed [2]. As for 3D image analysis, only object visualization [3] has been performed. However, to our knowledge landmine detection and classification using the 3D nature of GPR images is new.

The goal of this paper is to describe the developed algorithm that uses specific properties of these images to detect landmines. The algorithm should meet a number of demands:

- All recognizable landmines need to be detected.
- A low number of false alarms is required.
- Multiple 2D images are combined to form 3D images. In the algorithm all actual 3D image information is used for detection and classification.
- The performance of the algorithm should be validated based on actual GPR measurements.

The novelty of this paper is the development of an algorithm, which detect landmines in GPR images using their 3D nature.

In Section 2 the acquisition and preprocessing of the data is described including a short description of its properties. Section 3 presents the detection procedure for 3D GPR images. The classification procedure is addressed in detail in Section 4. The results and a discussion of the performance are given in Section 5. Finally, the paper ends with conclusions and some recommendations in Section 6.

2. Generation of the 3D GPR image and its properties

The measurement campaign for the acquisition of the measurement data [4] was performed on a dry sandy lane at the test facilities for landmine detection systems located at TNO Physics and Electronics Laboratory in The Hague, The Netherlands. During the measurement campaign the GPR system has been mounted on the relocatable scanner of the Delft University of Technology. It scans along one axis measuring A-scans every 1 cm and combines them to B-scans along the other axis with an interval of 1 cm as well. The measured area is 170 cm by 196 cm and 20 cm in depth. Two types of landmine simulants are buried there: PMN mines (metal content, diameter: 11.2 cm) and M14 mines (very low metal content, diameter: 5.6 cm). In total, 12 mines are buried (6 PMN mines and 6 M14 mines) and one unintentionally buried man-made object which radar image has such strong resemblance to that of a landmine that it is also labeled as a wanted target. Further, some false alarms like stones, a bottle and a piece of barbed wire are intentionally buried. All other objects are referred to as clutter and are unwanted in the detection and classification process.

The GPR system that was used to acquire the data is the polarimetric ultra-wideband (UWB) video impulse radar (VIR) system. This system has been developed by IRCTR

and is dedicated to buried landmine detection. The VIR system consists of 2 transmit antennas and 4 receive antennas as seen in Fig. 1. The data is measured in a co-polar antenna combination and with the receive antenna in "monostatic" and in "bistatic" mode. For further information about the VIR system one is referred to [5].

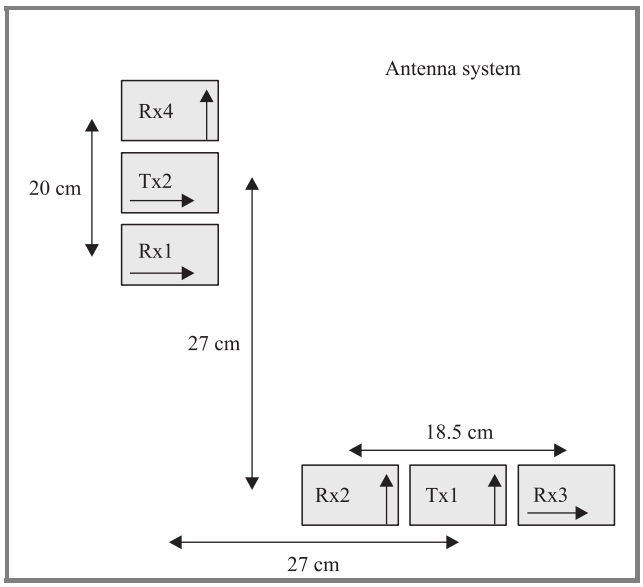

Fig. 1. Top view of the antenna system.

Before image processing is performed, the acquired data have to be preprocessed to remove system instabilities and to reduce clutter. The latter can be obtained by applying SAR processing using a three-dimensional imaging method. All performed preprocessing steps including the 3D imaging method are found in [6].

Properties of 3D radar images of wanted targets that discriminate them from clutter are used for detection and classification of these wanted targets. These are the rotationally symmetric amplitude distribution of wanted target images in horizontal cross section, the high amplitudes and the appearance in many depth slices (the total depth is sampled with a step of 0.25 cm resulting in 80 depth slices).

3. Object detection

Before object detection is applied, the envelope of each A-scan in the 3D image is computed. This is done to eliminate zero crossings and negative amplitudes in the time-domain signal. The phase of the envelope is not used, because such phase analysis (allowing for investigating discontinuities in permittivity) is beyond the scope of this work.

To detect the wanted targets in the 3D image, a threshold procedure is used. Instead of using a fixed threshold procedure, an adaptive threshold technique is used to establish different threshold values for each depth slice of the 3D image. The reason for using different thresholds is that the amount of clutter is much higher in depth slices containing residuals of the ground reflection than in other depth slices and therefore needs a higher threshold value to avoid detection of clutter.

The used adaptive threshold technique is called the decreasing threshold procedure. For each depth slice all possible threshold values are applied. For each threshold value, objects are grouped in the resulting binary depth slice; the number of these detected objects is computed and is plotted against the accompanying threshold value. The resulting curve is different for each depth slice, but it has roughly the same shape (Fig. 2). From experience, it turned out that

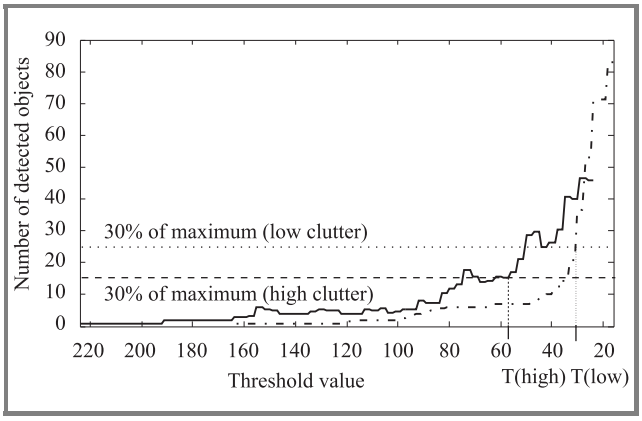

Fig. 2. Number of detected object images versus threshold value. The solid curve represents a depth slice with high amount of clutter, while the dashed curve is the result from a depth slice with low amount of clutter. The horizontal lines represent 30% of the maximum values of the curves with T(high) and T(low) as resulting threshold values.

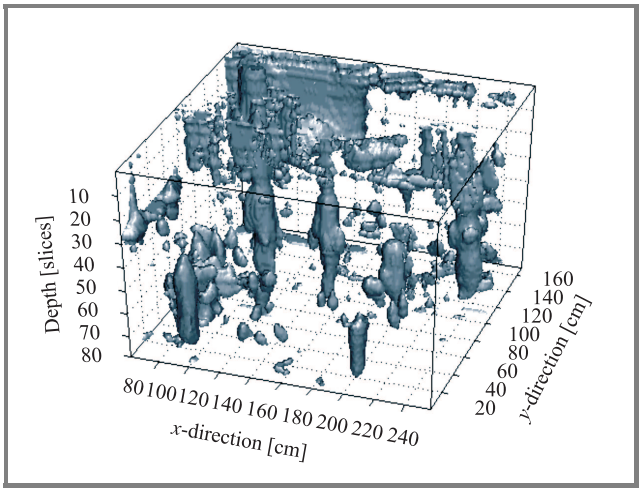

Fig. 3. Binary 3D image volume after threshold procedure.

the best threshold value is situated at the beginning of the steep slope in the curve. This threshold value can be found by calculating a percentage of the maximum number of detected objects in the curve and determine its accompanying threshold value. The choice for this percentage is based on the minimum size of the buried landmines in the measured area and is set to 30% of the maximum of the curve.

In Fig. 2 it is seen that for depth slices with a low amount of clutter the threshold value will be lower than for depth slices with a high amount of clutter.
The 3D binary result after applying the decreasing threshold procedure is shown in Fig. 3. Not only are the wanted targets detected, but also surface clutter and other unwanted objects. It is still difficult to distinguish the wanted targets from these unwanted objects and therefore classification is performed to eliminate the clutter and to obtain a low number of false alarms.

4. Object classification

Classification is based on the established properties of wanted targets. Because it is desirable to remove clutter objects before classification, size based clutter removal (Subsection 4.1) is applied. For classification of all remaining objects (Subsection 4.3), features are extracted from the established properties and selected (Subsection 4.2).

4.1. Size based clutter removal

Based on the dimensions of the wanted targets, two types of object removal are applied: removal of objects with a large horizontal size and removal of objects with a small height.

4.1.1. Removal of objects with a large horizontal size

Especially the residuals from the ground reflection result into detected objects with large horizontal dimensions. These are extremely unwanted for further processing and do not meet the dimension criteria for wanted targets. Therefore, these object images should be removed from the 3D image volume. The removal is performed per depth slice.
An unwanted secondary but slightly acceptable consequence is the possibility that wanted target images merged with clutter images in one or more depth slices are removed as well. To avoid this as much as possible, the horizontal size limit needs to be set with a sufficient margin.

4.1.2. Removal of objects with a small height

The most characteristic property of wanted targets is their appearance in many depth slices. The height of the wanted target images depends on the spatial length of the radar pulse in soil (vertical resolution), the sampling, the depth of the wanted targets (related to the intensity), the physical height of the wanted targets and the chosen threshold value for object detection.
The removal of object images with small height is performed by taking image slices in vertical directions along the *x*- and *y*-direction respectively and removing all objects smaller than an established height limit. This height limit is based on the height of the smallest and weakest wanted target image in the data.

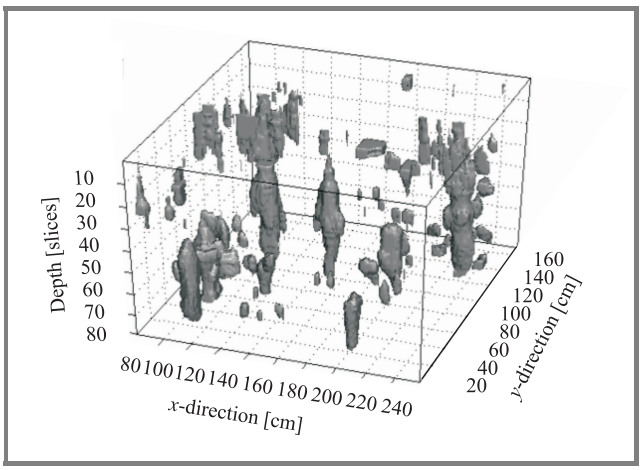

Fig. 4. Binary 3D image volume after size based clutter removal.

The overall result after the size based clutter removal is shown in Fig. 4, where the amount of detected clutter objects is decreased by 70% from 351 to 112 objects.

4.2. Feature extraction

Feature extraction is a preparatory step for the classification of the detected object images and has a big influence on the distinction of wanted target images from clutter images.
The features are divided into four categories: statistical, structure-, shape- and size-based features. Due to the earlier performed size-based clutter removal no features have been selected from the last category. The statistical and structure-based features are computed from intensity images and therefore require a 3D window to be placed around the detected objects [7]. The shape based features are computed from binary images.
The quality of a feature depends on its discriminating power, reliability and independency with other features. Based on these criteria, nine features (F_1 to F_9) are determined to be used in the feature selection:

Statistical based features

F_1 maximum intensity

F_2 ratio of mean over maximum intensity

F_3 ratio of minimum over maximum intensity

F_4 standard deviation

Structure based features

F_5 similarity with a template

F_6 similarity between orthogonal horizontal cross lines

F_7 depth similarity

Shape based features

F_8 eccentricity of the bounding ellipse

F_9 ratio of minor axis over major axis lengths

4.3. Classification

To limit the computational time, the best performing features of the total feature set are selected (with the so-called forward feature selection method [8]) to be used in the classification process.

The classifier is based on a simple classification rule. For testing of the classification routine the leave-one-out method is used to obtain training and test sets from the feature set without having a large amount of objects in this feature set. The classification boundary is calculated from the training set, which is then used to decide whether a test object is a wanted target or a clutter object. To minimize the risk of having a missed detection, the boundary is computed with a certain safety margin, which is 5% of the overall maximum value of the specific feature added to the boundary. In Fig. 5 scatter plots for two features are plotted including the computed boundaries, showing that the boundaries eliminate many clutter objects.

The selected feature set contains 5 features. These are: the maximum intensity (F_1), because wanted target reflections exhibit high amplitudes; the ratio of the mean over the maximum intensity (F_2); similarity with a template (F_5), where the template is a representative horizontal cross section of one of the wanted target images; similarity between orthogonal horizontal cross lines (F_6), because of the rotationally symmetric amplitude distribution of wanted target images in horizontal cross section; and the ratio of the length of the minor axis over that of the major axis (F_9), also because of the circular shape of the wanted target images.

After classification, 20 false alarm objects retain in the image volume as can be seen in Fig. 6. This corresponds to a clutter reduction of more than 80%.

Because of the limited down-range resolution, it is not possible to have two distinctive landmine reflection events in a depth range of 20 cm which are situated closer than the smallest possible distance between two landmines. Therefore, these object images have to be merged into one object image.

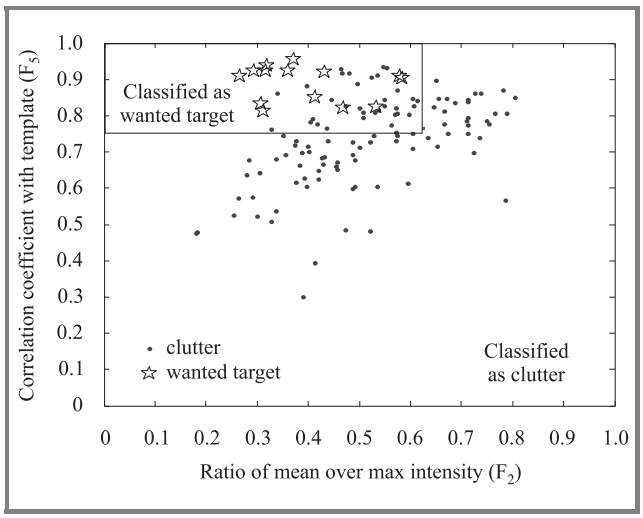

Fig. 5. Scatterplot of feature F_2 and F_5 including the classification boundary.

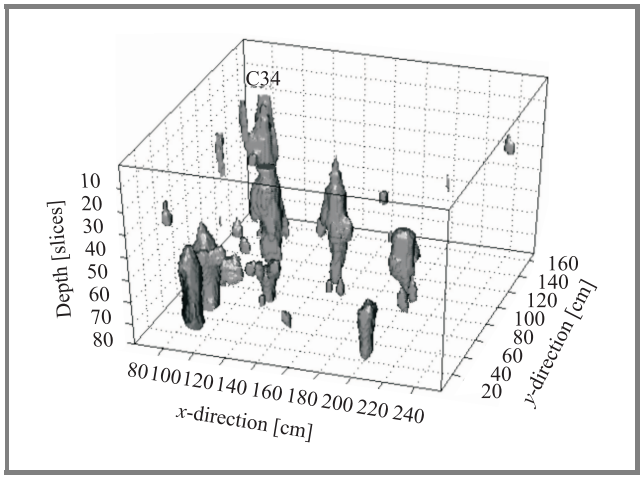

Fig. 6. Binary 3D image volume after classification.

5. Performance of the algorithm

Besides the requirement that 100% of all wanted targets have to be detected, the algorithm has to meet also another requirement which is the low amount of false alarms. In Fig. 7 the clutter reduction for each image processing procedure of the algorithm is shown. It is remarkable that the largest reduction of clutter is achieved by applying a size-based clutter removal; that is, the removal of objects with a small height (procedure *b*). The increase in amount of clutter objects in procedure a is due to division of objects into more objects by removing parts of objects with a large horizontal size per depth slice.

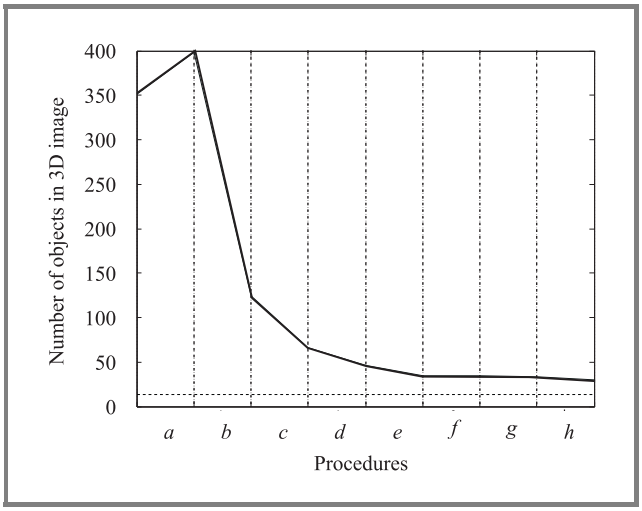

Fig. 7. Reduction of the amount of object images per procedure (solid line). The dashed line represents the number of the buried landmines in the test-lane area. Procedures are: *a*, *b* – size based clutter reduction; *c*, *d*, *e*, *f*, *g* – classification performance per feature; *h* – merging of objects due to down-range resolution.

The results of the classification method are shown in the confusion matrix of Table 1. It demonstrates that for

this 3D image the amount of clutter images classified as wanted targets (false alarms) has been drastically reduced to 18 including a positive detection of 12 wanted targets. All small M14 mines are classified as wanted target. The missed detection is an "easy to detect" PMN mine, which is situated close to the border of the measurement test-lane area. The misdetection is caused by incorrect SAR processing, which resulted in an oval shape for the landmine in horizontal cross section instead of a circular shape. For correct SAR processing some defined space around object images is required, which is not the case for objects situated near the border of the test lane area. This problem will be solved when the measurement area has an overlap with its neighboring measurement areas in such a way that incorrect SAR processing can be avoided.

Table 1
Confusion matrix of the classification results

Clutter	Classifier-determined label target	Classifier-determined label clutter
True wanted target	12	1
True clutter	18	93

The above reported results are obtained by using the leave-one-out-method to create larger training sets, but a consequence is that the test sets are not completely independent from the training sets. Therefore, the reliability of the established classification boundaries is tested with data from the other transmitting and/or receiving antennas. In total, 3 test sets are used; one where the receive antenna is also in "monostatic" mode as is the case for the training data and two sets with the receive antenna in "bistatic" mode. The results are put in confusion matrices, which are shown in Table 2.

Table 2
Confusion matrices for other transmitter/receiver combinations; transmit/receive numbering as indicated in Fig. 1

Bistatic mode Tx1Rx4		
Clutter	Classified wanted target	Classified clutter
True wanted target	2	5
True clutter	11	95
Monostatic mode Tx2Rx1		
Clutter	Classified wanted target	Classified clutter
True wanted target	7	1
True clutter	13	53
Bistatic mode Tx2Rx3		
Clutter	Classified wanted target	Classified clutter
True wanted target	7	3
True clutter	28	113

It can be seen that the classification results for the transmitter/receiver combinations in "bistatic" mode are worse than those for the "monostatic" mode. The large number of missed detections for "bistatic" mode has two main reasons. First of all, in "bistatic" mode the reflections are weaker. Therefore, classification which is partly based on intensity values of the object images causes more missed detections. Secondly, due to the large distance between the transmit and receive antenna in "bistatic" mode, the landmines are tilted with respect to the vertical direction. Therefore, the wanted target images do not fit the 3D window nicely anymore, which results in a larger number of missed detections.

The transmitter/receiver combination in "monostatic" mode of Table 2 has a reasonably low number of false alarms and almost all wanted targets are classified correctly. The reason for the one missed detection is its weak reflections. To conclude, the data measured in "monostatic" mode gives better results and satisfies the established classification boundaries more.

In view of the obtained results, we have to take into account that the data were measured over a fixed type of ground with two types of buried mines. When measuring over a lossy type of ground, the results probably will deteriorate.

Besides the circular shape of the buried landmines, other shapes are possible. This may change the properties of the landmine images. Consequently, in this case the features that are used in the here-presented classification scheme will probably not act properly, causing the performance of the classification procedure to degrade.

The size of the measured area also influences the performance of the procedures. Measuring a larger area results in more objects and therefore in a larger training set.

Points for improvement in the overall landmine detection procedure are the adaptive thresholding technique, the 3D window used in the classification procedure and the classification procedure itself.

6. Conclusions and recommendations

An algorithm for GPR landmine detection has been developed, where full use is made of the 3D nature of GPR images. It consists of two procedures: object detection based on a self-developed adaptive thresholding technique and object classification using a simple classification routine designed to reduce the possibility of missed detections. This algorithm has been realized, tested and validated.

Landmine detection in 3D GPR images gives promising results. All M14 mines are detected and classified as wanted target. Only one large PMN mine is misclassified due to incorrect SAR processing at the border of the measurement area. The removal of objects with a small height proves to be a good procedure to eliminate clutter from the image volume. However, we have to implement this procedure with care to avoid that small and deeply buried landmines are removed.

The now-available object detection procedure also needs an expert decision; however in future this decision could be determined by the size and possible depth of the buried landmines.

The classifier in the object classification procedure is quite simple, but effective. When paying more attention to the selection of the classification method, it might be better to use a neural network as classifier, which "learns" to separate landmines from clutter based on their radar images.

The performance of a landmine detection system is also improved sensor fusion. Merging different sensors like the metal detector, the infrared detector and GPR into one landmine detection system [2] leads to the necessary further development of algorithms with improved performance.

References

[1] A. G. Yarovoy, V. Kovalenko, F. Roth, L. P. Ligthart, and R. F. Bloemenkamp, "Multi-waveform full-polarimetric GPR sensor for landmine detection: first experimental results", in *Int. Conf. Requir. Technol. Detect., Remov. Neutr. Landm. UXO*, Brussels, Belgium, 2003, pp. 554–560.

[2] F. Cremer, W. de Jong, and K. Schutte, "Fusion of polarimetric infrared features and GPR features for landmine detection", in *2nd Int. Worksh. Adv. GPR*, Delft, The Netherlands, 2003, pp. 222–227.

[3] L. Zanzi, M. Lualdi, H. M. Braun, W. Borisch, and G. Triltzsch, "An ultra high frequency radar sensor for humanitarian demining tested on different scenarios in 3D imaging mode", in *9th Int. Conf. Ground Penetr. Radar, Proc. SPIE*, vol. 4758, pp. 240–245, 2002.

[4] A. G. Yarovoy, V. Kovalenko, F. Roth, J. van Heijenoort, P. Hakkaart, W. de Jong, F. Cremer, J. B. Rhebergen, P. J. Fritz, M. A. Ouwens, and R. F. Bloemenkamp, "Multi-sensor measurement campaign at TNO-FEL test lanes in July 2002", in *Int. Conf. Requir. Technol. Detect., Remov. Neutr. Landm. UXO*, Brussels, Belgium, 2003, pp. 208–215.

[5] A. G. Yarovoy, L. P. Ligthart, A. Schukin, and I. Kaplun, "Polarimetric video impulse radar for landmine detection", *Subsurf. Sens. Technol. Appl.*, vol. 3, no. 4, pp. 271–293, 2002.

[6] J. Groenenboom and A. G. Yarovoy, "Data processing and imaging in GPR system dedicated for landmine detection", *Subsurf. Sens. Technol. Appl.*, vol. 3, no. 4, pp. 387–402, 2002.

[7] E. E. Ligthart, "Landmine detection in high resolution 3D GPR images", M.Sc. thesis, Delft University of Technology, Faculty of Electrical Engineering, Mathematics and Computer Science, Delft, The Netherlands, 2003.

[8] A. R. Webb, *Statistical Pattern Recognition*. London: Hodder, Arnold, 2001.

Eveline E. Ligthart was born in Leiden, The Netherlands, on February 18, 1979. She received the M.Sc. degree in electrical engineering from the Delft University of Technology, The Netherlands, in March 2004. The present paper is part of her graduation thesis "Landmine detection in high resolution 3D GPR images" performed at the International Research Centre for Telecommunications and Radar (IRCTR). At present, she is a pattern recognition scientist at Prime Vision in Delft, The Netherlands. Her work includes the recognition of postal addresses and license plates.

e-mail: E.Ligthart@PrimeVision.com
International Research Centre
for Telecommunications and Radar (IRCTR)
Faculty of Electrical Engineering,
Mathematics and Computer Science
Delft University of Technology
Mekelweg st 4
2628 CD Delft, The Netherlands

Alexander G. Yarovoy graduated from the Kharkov State University, Ukraine, in 1984 with the diploma with honor in radio physics and electronics. He received the Cand. phys. and math. sci. and Dr. phys. and math. sci. degrees (all in radio physics) in 1987 and 1994, respectively. In 1987 he joined the Department of Radiophysics at the Kharkov State University as a Researcher and became a Professor there in 1997. From September 1994 through 1996 he was with Technical University of Ilmenau, Germany, as a Visiting Researcher. Since 1999 he is with the International Research Centre for Telecommunications and Radar (IRCTR) at the Delft University of Technology, The Netherlands, where he coordinates all GPR-related projects. Currently his main research interests are in ultra-wideband technology including radars and in applied electromagnetics.

e-mail: A.Yarovoy@EWI.TUDelft.nl
International Research Centre
for Telecommunications and Radar (IRCTR)
Faculty of Electrical Engineering,
Mathematics and Computer Science
Delft University of Technology
Mekelweg st 4
2628 CD Delft, The Netherlands

Friedrich Roth was born in Munich, Germany, in 1972. He received a M.Sc. degree in geophysics from the Colorado School of Mines (CSM), USA, in 1999. While at CSM, he studied the possible use of inertial navigation for real-time antenna position and orientation estimation for ground penetrating radar data acquisition. Since 2000 he has been a Ph.D. student at the International Research Centre for Telecommunications and Radar (IRCTR) at the Delft University of Technology, The Netherlands, working on landmine detection problems. His current research interests include electromagnetic scattering

from buried landmines, deconvolution and target identification, GPR polarimetry, and real-time data processing.
e-mail: FRoth@Clamart.oilfield.slb.com
International Research Centre
for Telecommunications and Radar (IRCTR)
Faculty of Electrical Engineering,
Mathematics and Computer Science
Delft University of Technology
Mekelweg st 4
2628 CD Delft, The Netherlands

Leo P. Ligthart was born in Rotterdam, the Netherlands, on September 15, 1946. He received an engineer's degree (*cum laude*) and a Doctor of technology degree from Delft University of Technology in 1969 and 1985, respectively. He is Fellow of IEE and IEEE. He received doctorates (*honoris causa*) at Moscow State Technical University of Civil Aviation in 1999 and Tomsk State University of Control Systems and Radioelectronics in 2001. He is academician of the Russian Academy of Transport. Since 1988, he has held the chair of Microwave Transmission, Radar and Remote Sensing in the Faculty of Electrical Engineering, Mathematics and Informatics, Delft University of Technology. In 1994, he became Director of the International Research Centre for Telecommunications and Radar. Prof. Ligthart's principal areas of specialization include antennas and propagation, radar and remote sensing, but he has also been active in satellite, mobile and radio communications. He has published over 350 papers and 1 book.
e-mail: L.P.Ligthart@IRCTR.TUDelft.nl
International Research Centre
for Telecommunications and Radar (IRCTR)
Faculty of Electrical Engineering,
Mathematics and Computer Science
Delft University of Technology
Mekelweg st 4
2628 CD Delft, The Netherlands